Colloid Polym Sci 276:144–151 (1998)

ORIGINAL CONTRIBUTION

M.S. Sfiligoj
P. Zipper

WAXS analysis of structural changes of poly(ethylene terephthalate) fibers induced by supercritical-fluid dyeing

Received: 14 May 1997
Accepted: 23 September 1997

M.S. Sfiligoj[1] (✉) · Prof. Dr. P. Zipper
Institute of Physical Chemistry
University of Graz
Heinrichstrasse 28
A-8010 Graz
Austria

[1]Textile Chemistry Institute
University of Maribor
Smetanova 17
2000 Maribor
Slovenia
E-mail: majda.sfiligoj@uni-mb.si

Abstract Supercritical CO_2 fluid, a new environmentally friendly dyeing medium, changes the fiber structure to a certain extent in dependence on the treatment temperature and pressure used. Therefore the changes of crystalline structure in poly(ethylene terephthalate) (PET) fibers as brought about under the influence of supercritical CO_2 fluid were investigated.

For the data collection of wide-angle X-ray diffraction full patterns a two-circle goniometer, equipped with a position sensitive detector, was used. From the observed two-dimensional fiber diffraction patterns the crystallinities of various treated fibers were evaluated. The equatorial scanning yielded the dimensions of crystallites. To elucidate the fiber-surface morphology changes SEM analyses were performed.

The supercritical fluid dyeing of PET fibers with highly developed microfibrillar structure under taut-ends conditions promotes changes which are characterized by an increase in crystallinity and by diminution of the apparent crystallite dimensions. Some changes of surface morphology of dyed fibers were observed as well.

Key words Poly(ethylene terephthalate) (PET) fibers – supercritical-fluid (SCF) dyeing – wide-angle X-ray scattering (WAXS) – scanning electron microscopy (SEM)

Introduction

It is well known that the morphology of semicrystalline polymers depends on their thermal history and a considerable amount of research has been carried out on the effect of heat-treatment on the structure and mechanical properties of poly(ethylene terephthalate) (PET). Oriented and glassy PET structures change their supramolecular structure easily during annealing and mechanical loading [1], while semicrystalline PET materials possess lower deformability [2].

Thermal treatment of PET semicrystalline fibers changes the fiber fine structure in dependence on the conditions applied. Changes in structure during thermal contraction of drawn PET fibers can be summarized as a decrease in long period, a decrease in amorphous orientation function, an increase in the regular chain folding, an improvement in the lateral order in the crystallites, an increase in the electron density difference between the crystalline and amorphous domains and an increase in the lateral order of the macrolattice [3]. Superheated steaming of the fibers increases their shrinkage, crystallinity and crystallite size and decreases their dyeability compared to dry heat treatment [4].

Free-annealed and taut-annealed samples show considerable differences [5]. There is in general a decrease in crystalline orientation with increase in heat-setting temperature in free-annealed samples and an increase in the case of the taut-annealed fibers, but in both sets of samples

the degree of crystallinity and the crystal size increase. By the heat treatment a decrease in birefringence of free-annealed samples and an increase for taut-annealed samples was observed [5].

The consequence of the thermal treatment of low-shrinkage PET fibers under free-ends conditions in amorphous domains is a conformational transition from trans to gauche, which causes chain coiling and loss of orientation of the chains of the original material that is characterized by a high amount of trans with highly oriented and extended segments [6].

In the 1980s supercritical fluid (SCF) received widespread applications. Introduction of supercritical fluids as transport media for hydrophobic dyes in SCF dyeing processes [7] has many advantages to offer: no waste water, shorter dyeing times, no auxiliaries are required, a reductive washing off is unnecessary, because the dyestuff which is not absorbed is removed with the supercritical fluid, the drying process is omitted, surplus dyestuff and fluid can be reused. Carbon dioxide with advantageous critical conditions, safety and physiological properties is most suitable for the processes at supercritical conditions. Dyeing in supercritical CO_2 is carried out analogous to aqueous systems. Both decisive tasks of water at dyeing, which means the transport of dyestuff and heat to the fibre, are in the new dyeing process replaced with supercritical fluids [7].

Recently, the effect of supercritical carbon dioxide dyeing conditions on the morphology of PET fibers was studied by Drews [8]. The techniques applied comprised scanning electron microscopy, cross-sectional analysis, optical birefringence, tensile tests, DSC, and dynamic mechanical thermal analysis. Supercritical CO_2 exposed fibers were found to change their mechanical properties, although no significant differences in the fiber morphology could be observed [8].

In order to gain more insight into the influence of supercritical fluids (SCF) on the crystalline structure of PET fibers we performed wide-angle X-ray scattering (WAXS) and scanning electron microscopy (SEM) studies on specimens treated under supercritical CO_2 fluid. The treatment without the dyestuff (blind dyeing) corresponded to the supercritical fluid dyeing (SCD) conditions conventionally used in practice.

Experimental

Sample preparation

A PET multifilament yarn with a linear density of 143 dtex[1] with a highly developed fibrillar structure was used. The intrinsic viscosity of the PET polymer was 0.71 g/l and the take up velocity 3000 m/min. The drawing of the fibers was carried out at 523 K with a draw ratio of 1:2.5. The heat setting temperature was 523 K with the permitted shrinkage of 20%.

The unmodified poly(ethylene terephthalate) samples wound on a perforated cylinder were treated in supercritical CO_2 fluid (critical conditions $T_c = 304.2$ K, $p_c = 7.38$ MPa [7]) under different conditions. The dyeing autoclave was preheated and when the working temperature was reached, CO_2 was isothermally compressed to the required pressure. The dyeing isobaric and isothermal period was followed by a stepwise expansion to avoid deposits of excessive dyestuff forming on the surface of the fabric if the dyestuff would be used. The treatment temperature used was 353, 393, 403 and 423 K, the treatment time 60 or 10 min and the pressure 10, 25 and 40 MPa, respectively. The treatment conditions were adapted to the supercritical fluid dyeing conditions conventionally used [7].

Analytical methods

Wide-angle intensity curves were obtained on a diffractometer Siemens D500 using symmetrical reflection geometry. Nickel-filtered copper radiation (CuK_α, $\lambda = 0.1542$ nm) was used for all X-ray experiments. The distribution of the scattering intensity on the equator was scanned over the range of $2\theta = 10^\circ$ to $2\theta = 35^\circ$ in steps of 0.1°. The measuring time for each point was 20 s. The scattering was corrected for polarization factor and absorption. The corrected scattering curves were modelled by Pearson VII functions with the peak shape parameter taken as 2.5 for the crystalline reflections and 100 for the amorphous halo. The crystallinity was determined in the form of a crystallinity parameter defined as the ratio of the integrated intensity under the crystal reflections and the integrated total scattering intensity. This procedure was chosen because of the good reproducibility of results, but it does not include any correction for lattice distortions [10–14].

The apparent size of crystallites perpendicular to the planes (hkl) was determined by the Scherrer equation [15, 16]:

$$D_{(hkl)} = \frac{K\,\lambda}{\beta \cos\theta}\,. \tag{1}$$

$D_{(hkl)}$ is the crystallite size, K a proportionality factor (0.9), λ the applied wavelength, β a measure of the line width (full-width at half-maximum, in rad) and θ Bragg's angle.

[1] tex = g/km; a unit for describing the fineness of textile fibres [9].

A correction of β for instrumental broadening was not performed because only the changes of $D_{(hkl)}$ upon treatment were of interest.

To take into account also the contribution of non-equatorial reflections, the crystallinity parameter was additionally determined from two-dimensional scattering diagrams, which were obtained by means of a two-circle goniometer. The intensity was scanned in normal transmission geometry over an azimuthal angular range from 0° to 180° (in steps of 2.5°) using a linear position sensitive detector (PSD) for registration. The full pattern was recorded in form of 73 curves in two parts, with the detector fixed at 22° for the range from $2\theta = 8°$ to $2\theta = 36°$ and at 37° for the range from $2\theta = 23°$ to $2\theta = 51°$, respectively. The measuring time per curve was 420 s. The agreement of the two parts of the diagram was very good as shown for the overlap of both equatorial curves (Fig. 1). The fusion of both parts of the scattering diagram was performed at a scattering angle of 27°. Crystalline reflections for a supercritical CO_2 treated sample in the azimuthal range from 0° to 180° (scattering angular range from 10° to 51°) are presented in Fig. 2. A spherically averaged scattering curve was obtained by a weighted integration of the two-dimensional diagram [17].

The obtained "randomized" scattering $I(2\theta)$ curve was corrected for polarization factor, absorption and Compton scattering, yielding the coherent intensity. For the separation of the scattering diagram ($2\theta = 11.5°$ to $2\theta = 35°$), a polynomial approximation of degree 5 was used for the contribution of the amorphous phase. A small linear background scattering was additionally subtracted (Fig. 3).

A JEOL JSM 840A scanning electron microscope was used for direct observation of the supercritical fluid dyed samples. Before inspection, the fibers were coated according to the standard method for textile fibers to improve the low conductivity.

Results and discussion

The position of the three equatorial diffraction peaks due to the (0 1 0), (1 $\bar{1}$ 0) and (1 0 0) planes is $2\theta = 17.5°$, 22.5° and 25.8°, respectively. The diffractograms referring to the untreated sample and a SCF-dyed sample (403 K, 40 MPa) are shown in Figs. 4 and 5.

The crystallinity parameters, as deduced from the equatorial intensity distribution and from the X-ray full patterns (cf. Fig. 6) are considerably different, however, the same relative relations between various treated samples are obtained by means of both X-ray techniques. The non-random orientation of the crystallites in the samples

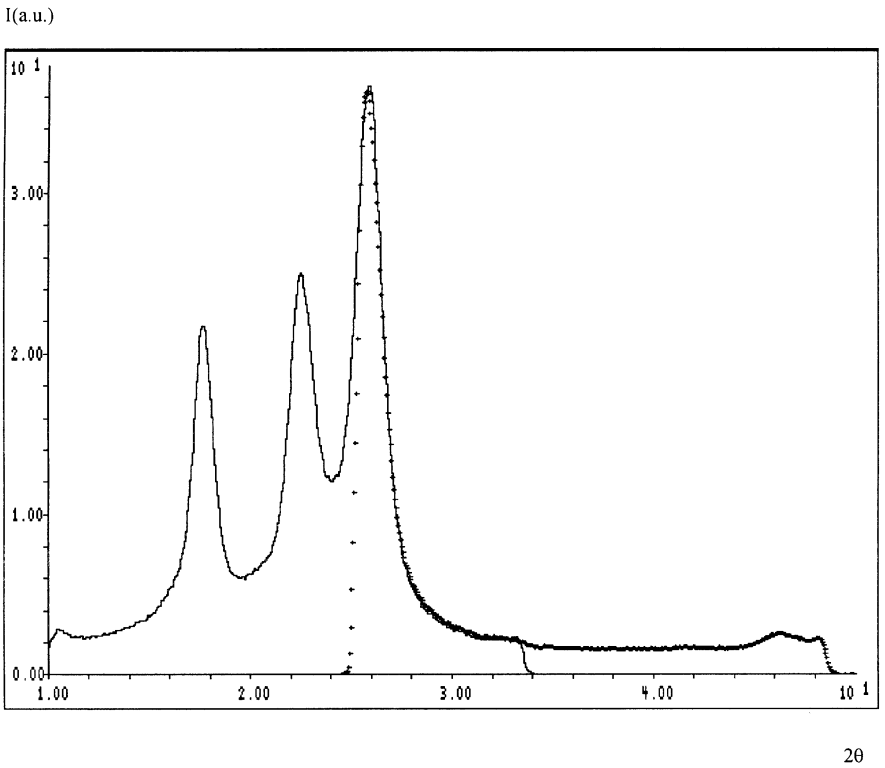

Fig. 1 Equatorial scattering, in the angular range of 2θ from 10° to 51°, recorded in two parts

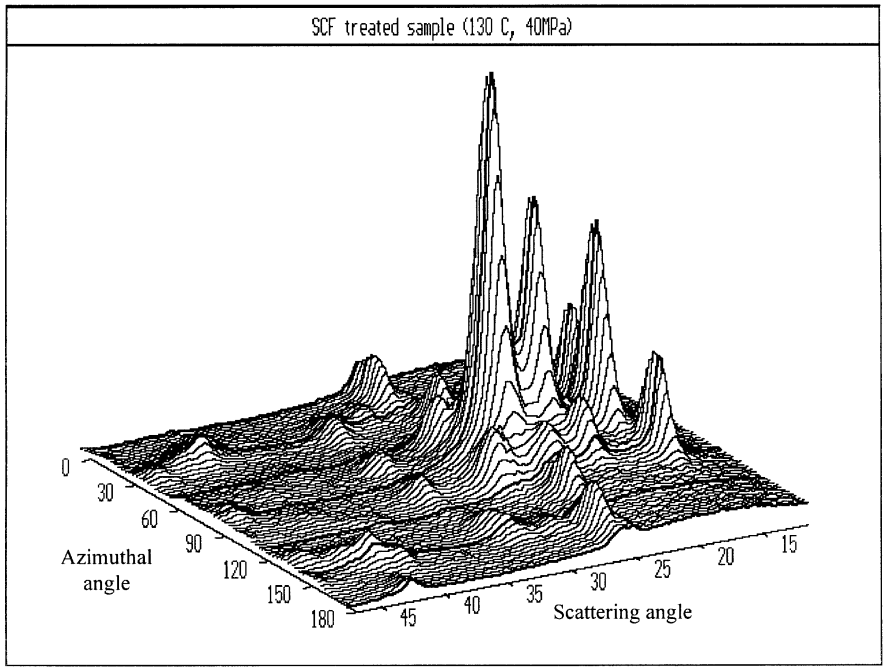

Fig. 2 Two-dimensional pattern of SCF-dyed PET fibers

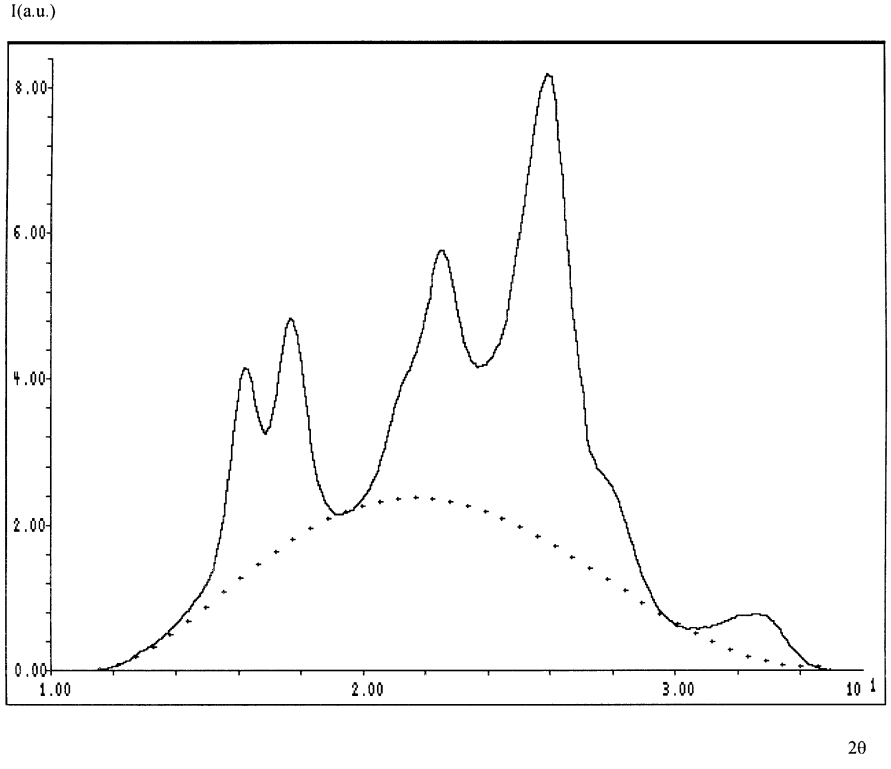

Fig. 3 The separation of the coherent scattering curve of the SCF treated sample. The area under the dotted line corresponds to amorphous diffuse scattering. The linear background has already been subtracted

gives rise to the higher crystallinity parameter obtained from the scans on the equator. For an isotropic polymer sample the X-ray diffraction intensity is a function of the scattering angle 2θ only, but for oriented fibers the X-ray intensity also depends upon the orientation of the sample due to the non-random orientation distribution of the various structural elements. For the crystallinity parameter determination from the two-dimensional patterns

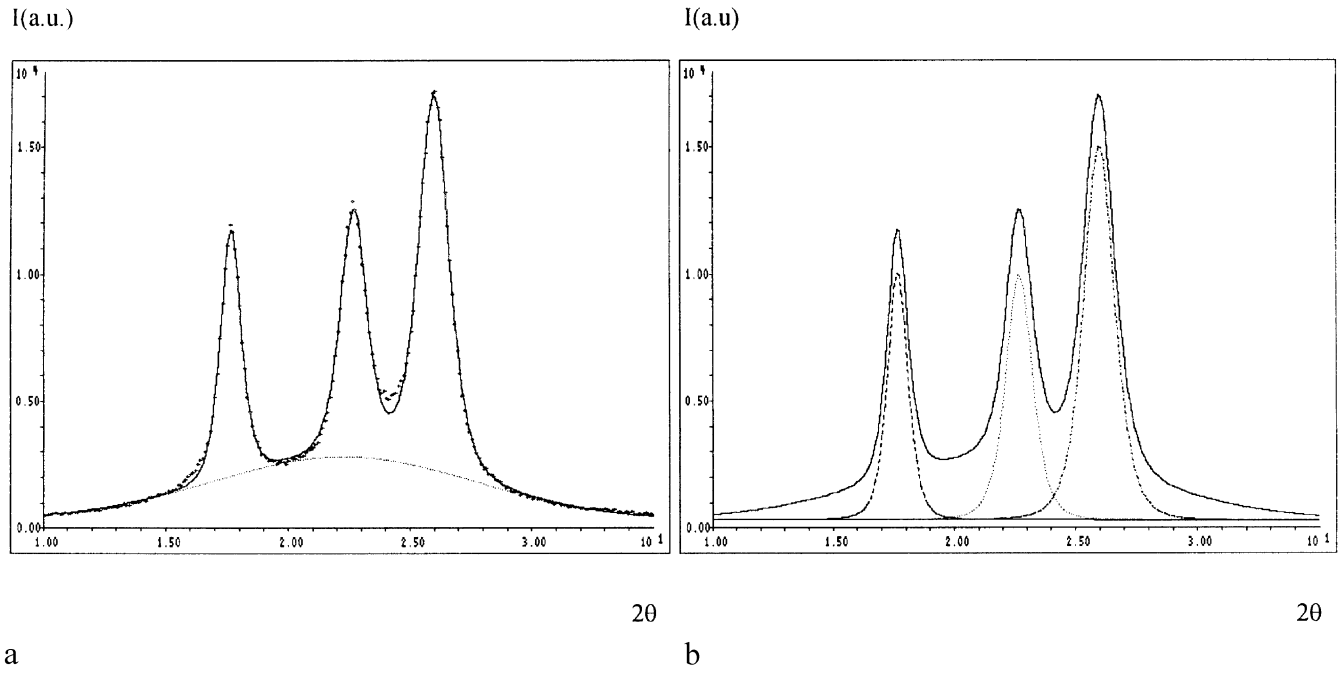

Fig. 4 Equatorial intensity profiles of the (0 1 0), (1 $\bar{1}$ 0) and (1 0 0) reflections of the untreated sample: (a) experimental and model curve with amorphous halo; (b) separation of the crystalline reflections of the model curve into Pearson VII functions

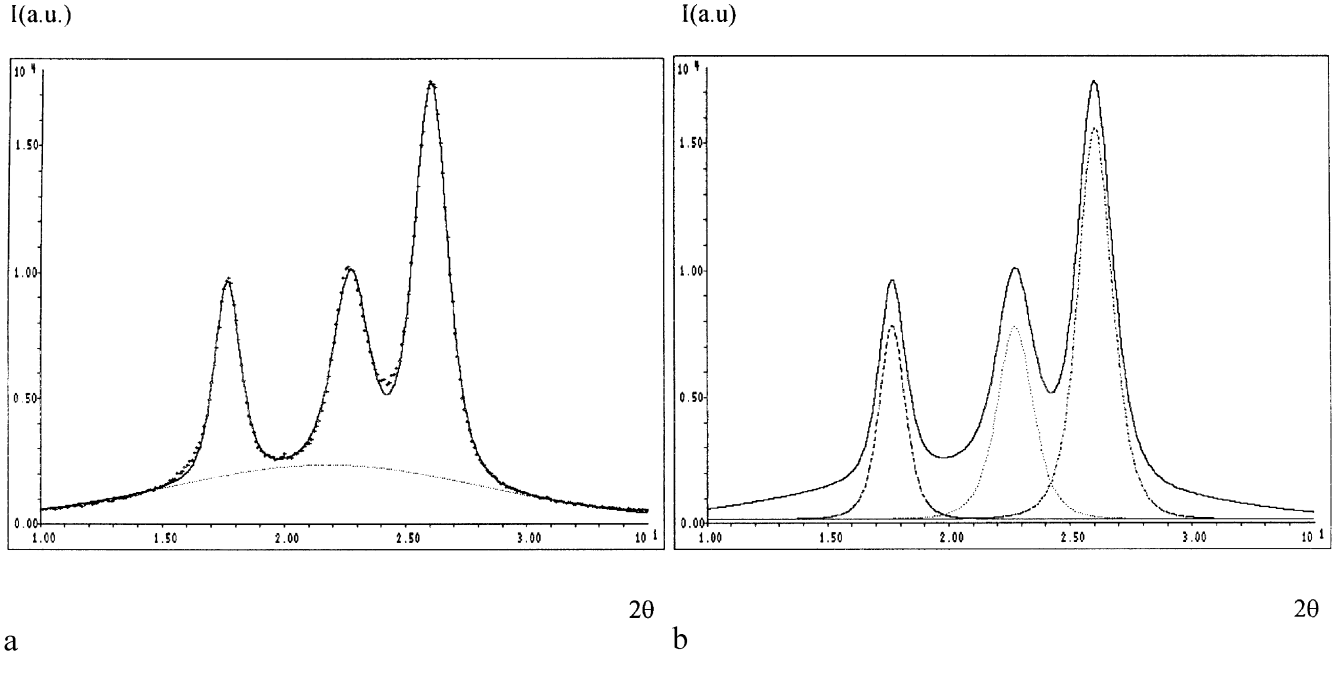

Fig. 5 Equatorial intensity profiles of the (0 1 0), (1 $\bar{1}$ 0) and (1 0 0) reflections of a SCF treated sample: (a) experimental and model curve with amorphous halo; (b) separation of the crystalline reflections of the model curve into Pearson VII functions

this dependency is averaged out [17]. Thereby the contribution of various non-crystalline structures to the amorphous scattering becomes larger and the ratio between the crystalline and total scattering is decreased.

The effects of blind-dyeing of the PET fibers in SCF are significant. From the two-dimensional patterns a crystallinity parameter of 0.47 was determined for the untreated PET sample. By the SCF treatment the crystallinity

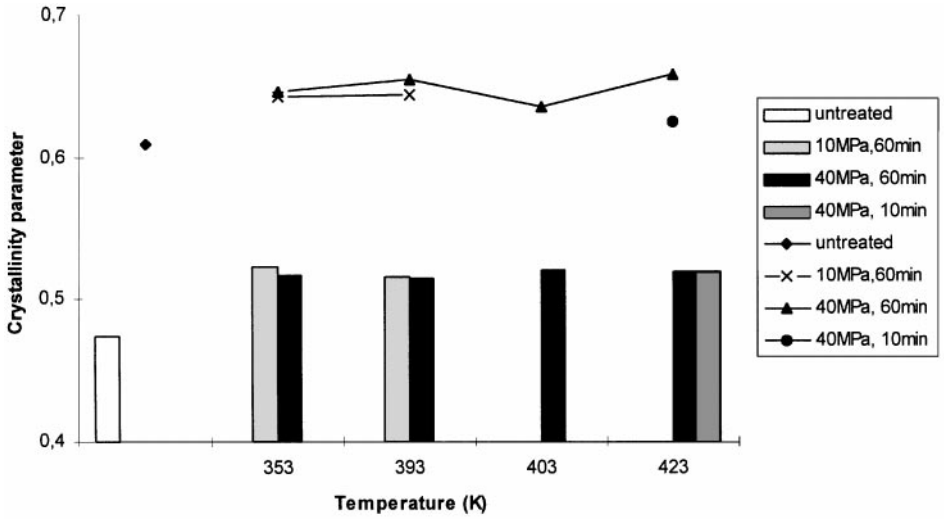

Fig. 6 Crystallinity parameter of the untreated and in SCF blind dyed samples, respectively, determined from the two- dimensional patterns (columns) and from the equatorial reflections (symbols)

parameter is increased for approximately 10%. As all the treatments were performed above the glass transition temperature of PET fibers and because the SCF lowers T_g of PET by about 20°–30° [18], the mobility of amorphous macromolecules becomes high enough to form some new crystallites although they are possibly smaller than the crystallites formed by the previous heat setting at the considerably higher temperature. Different treatment conditions show no difference with respect to the observed increase in crystallinity. The variation between the results obtained for various treated samples is about 1%. The changes arisen in the fibers are independent of the length of the dyeing period. It seems that the main factor causing the crystallinity increase is the elevated temperature, but as the treatment conditions were adapted to the conditions typically used in supercritical dyeing, the treatment temperature is obviously too low to cause appreciable differences between different treated samples. The observed crystallinity parameter changes were confirmed by the results obtained from DSC measurements [19].

Apparent crystallite sizes were determined from the reflection profiles for planes (*hkl*) as obtained from the resolution of the equatorial scattering curves into three Pearson VII functions. No correction for profile broadening due to lattice distortions was performed. The width of the crystalline reflection was found quantifiably changed after blind-dyeing, the observed changes correspond to a decrease of the apparent crystallite dimensions (cf. Table 1). The diminishing of crystallite sizes by thermal treatment of low shrinkage PET fibers (LSPF) with well-developed crystalline structure was also observed by Rodriguez et al. [6]. The thermal treatment of LSPF samples of high microfibrillar superstructure at intermediate temperatures (between 353 and 413 K) caused a reduction of crystallite dimensions which was brought about by certain fragmentation of the crystallites. Coiling of the amorphous macromolecules affected the crystallite structure by the formation of crystal imperfections and that was considered as a certain degree of fragmentation. Above the intermediate thermal conditions the perfection and size of crystallites was increased again [6].

Table 1 Apparent sizes of crystallites

Dyeing conditions T [K]; p [MPa]; t [min]	D_{010} [nm]	$D_{1\bar{1}0}$ [nm]	D_{100} [nm]
Untreated	8.2	6.4	5.6
353, 10, 60	6.4	4.8	5.1
353, 40, 60	6.2	4.6	5.1
393, 10, 60	6.5	4.9	5.2
393, 40, 60	6.2	4.6	5.1
403, 40, 60	6.3	4.7	5.1
423, 40, 60	6.5	4.8	5.1
403, 25, 10	6.5	4.9	5.1

A similar behavior was observed also with the samples treated in SC CO_2 fluid. Therefrom we can infer that the structural model for explanation of the crystalline changes could be alike. Thermally induced motions of the amorphous macromolecules tend by their coiling to form new crystallites. The usual fiber-model is composed of alternately crystalline and amorphous regions, with the molecules running through successive crystalline and amorphous regions. The growth of new crystallites during annealing increases the stress on the remaining part of the stretched macromolecular chain in the crystalline phase by pulling it and could cause its uncoiling on certain positions

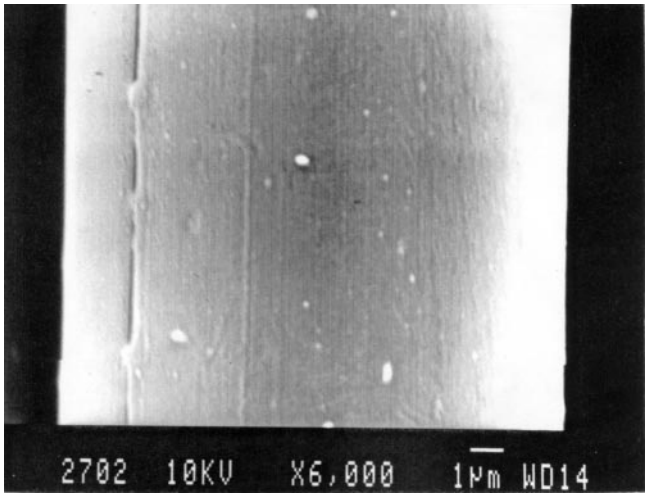

Fig. 7 SEM photograph of the untreated PET sample at a magnification of 6000×

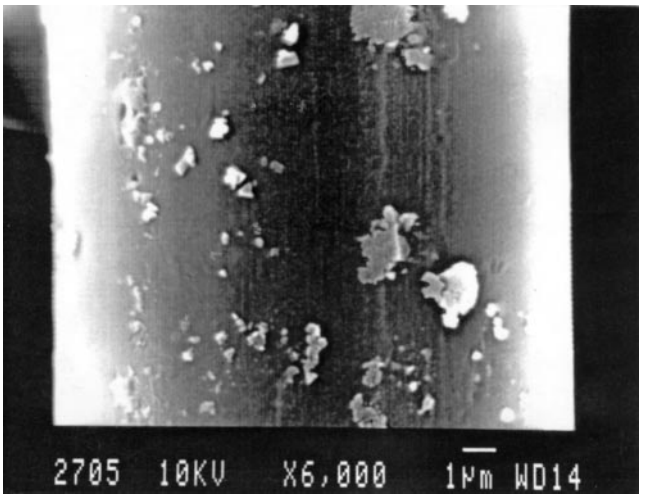

Fig. 8 SEM photograph of a SCF treated sample (treatment conditions: $T = 423$ K, $p = 40$ MPa; $t = 60$ min)

in the crystallites. Thereby imperfections in the crystallites are increased. This appearance is slightly intensified by the fibers' taut position during the SCF dyeing. The defects in the crystallites give the impression of smaller crystallites, what is reflected in the increased width of the crystalline reflections.

An additional influence on the formation of imperfections in crystallites could be observed also with the SCF dyeing at higher pressures. A slightly higher reduction of the crystallite dimensions was observed at the same temperature with the fibers treated at a higher pressure. In the case of SCD at 423 K and 40 MPa the relatively high temperature annihilated the influence of the higher pressure.

The apparent crystallite sizes perpendicular to the (1 0 0) planes are only slightly changed after the SCF process, whereas the relative changes of the crystallite dimensions perpendicular to the (0 1 0) plane and to the $(1\,\bar{1}\,0)$ plane are approximately equal, but significantly greater than the size reduction along the crystallite axis *a*. Huisman and Heuvel [20] reported that $D_{0\,1\,0}$ registers a greater growth than $D_{1\,0\,0}$ because the 0 1 0 direction is one in which the intermolecular interactions between ester dipoles exist and consequently this is likely the direction of crystallite growth by chain folding.

SEM photographs of the untreated PET sample and then treated under extreme conditions, taken at a magnification of 6000×, are presented in Figs. 7 and 8. The surface morphology of the fibers is remarkably changed after the dyeing process. Oligomer migration from the inner part of the fiber to the surface is clearly observed on the photographs, formation of oligomer crystals may be assumed (cf. ref. [8]). Small angle X-ray analyses of SCF treated PET fibers, unveiling an increase in the volume of the microvoid system, point in the same direction [21].

Conclusions

Unmodified PET fibers were blind-dyed in SC CO_2 fluid under various conditions. The effect of SCF dyeing on the fine structure of PET fibers was followed by means of WAXS and SEM. It was found that supercritical CO_2 fluid increases the total crystallinity of the polymer fiber. This may be explained by the formation of new crystalline regions because of the elevated temperature. The concomitant decrease of apparent crystallite dimensions suggests that the new crystallites are smaller or less perfect, however, a diminution of the size and an increase of imperfection of the previously formed crystallites may contribute as well. The change in crystallite dimensions is only slightly influenced by the high pressure used at the supercritical CO_2 fluid blind-dyeing. Some oligomers from the inner part of the fibers are pushed by the elevated pressure to the fiber surface and at their previous place new microvoids are formed. The main parameter effecting the changes in crystalline structure is the temperature, while the medium used shows less influence. The observed structural changes were additionally conditioned by the highly microfibrillar structure of the PET samples dyed in the SCF.

Acknowledgements Majda Sfiligoj Smole is grateful for the ARGE Alpen-Adria financial support from Land Steiermark, Austria.

References

1. Göschel U (1996) Polymer 37:4049–4059
2. Huang B, Ito M, Kanamoto T (1994) Polymer 35:1329–1331
3. Prevoršek DC, Tirpak GA, Harget PJ, Reimschuessel AC (1974) J Macromol Sci Phys B 9(4):733–759
4. Han L, Wakida T, Takagishi T (1987) Text Res J :519–522
5. Gupta VB, Kumar S (1981) J Appl Polym Sci 26:1865–1876
6. Rodriguez-Cabello JC, Santos J, Merino JC, Pastor JM (1996) J Polym Sci Part B; Polymer Phys 34:1243–1255
7. Knittel D, Saus W, Schollmeyer E (1993) J Text Inst 4:534–552
8. Drews MJ, Jordan C (1994) AATC, Book of Papers. USA, pp 261–272
9. Morton WE, Hearle JWS (1993) Physical Properties of Textile Fibres. The Textile Institute, Manchester
10. Ruland W (1961) Acta Crystallogr 14:1180–1185
11. Statton WO (1963) J Appl Polym Sci 7:803–815
12. Dumbleton JH, Bowles BB (1966) J Polym Sci A:951–958
13. Wlochowicz A, Jeziorny A (1972) J Polym Sci, Part A-2 10:1407–1414
14. Hindeleh AM, Johnson DJ (1978) Polymer 19:27–32
15. Bodor G (1991) Structural Investigation of Polymers. Ellis Horwood, New York
16. Alexander LA (1969) X-ray Diffraction Methods in Polymer Science. Wiley Interscience, New York
17. Desper CR, Stein RS (1967) Polym Lett 5:893–900
18. Saus W, Knittel D, Schollmeyer E (1993) Text Res J 63:135–142
19. Sfiligoj Smole M, Zipper P, Jeler S (1996) 6th European Polymer Federation Symp on Polymeric Materials EPF96, Book of Abstracts
20. Huisman R, Heuvel HM (1978) J Appl Polym Sci 22:943–965
21. Sfiligoj Smole M, Zipper P, Jeler S (1997) Progr Colloid Polym Sci 105: 85–90